

Chapter 6

Nuclear Overhauser effect

Contents

6.1. Introduction	163
6.2. Steady state NOE	165
6.2.1. Steady state NOE in real life	167
6.2.2. Selective and non-selective T_1	168
6.2.3. Steady state NOE in paramagnetic compounds	170
6.3. Truncated NOE	176
6.4. Transient NOE	178
6.5. NOE in the rotating frame (ROE)	180
References	183

6.1. Introduction

We have chosen to dedicate a full chapter to the nuclear Overhauser effect [1,2] (NOE) because its comprehension is of fundamental importance in dealing with nuclear relaxation [3,4]. Especially in paramagnetic compounds, it still represents a most powerful technique to detect dipolar connectivities; finally it allows the comprehension of two-dimensional spectroscopies based on dipolar coupling. NOE is the fractional variation of the intensity of a signal when another signal is selectively saturated.

The first application to paramagnetic compounds appeared in 1983 on signals with T_1 of the order of 50 ms: they were aliphatic residues in the active cavity of met-myoglobin cyanide which contains low spin iron(III) [5]. Soon it became apparent that the larger the molecular size, the larger the reorientational correlation time and the larger the NOEs. It was possible then to measure NOEs between signals with T_1 shorter than 10 ms with linewidths of several hundred hertz (at half-height) as long as the distances were small, as for geminal protons. This increased the number of successful applications of the NOE technique in the field of metallo-proteins. In the meantime, improvements were made in the difference spectra techniques, which permit the recording of the FID when a given signal is saturated and the subtraction of the FID when it is not (see Section 9.3.2); this is then repeated a number of times and the differences summed up. The baseline remains flat and small NOEs can be detected even under a large envelope of signals. When no NOE is observed, from the signal to noise ratio of the difference spectrum we can estimate

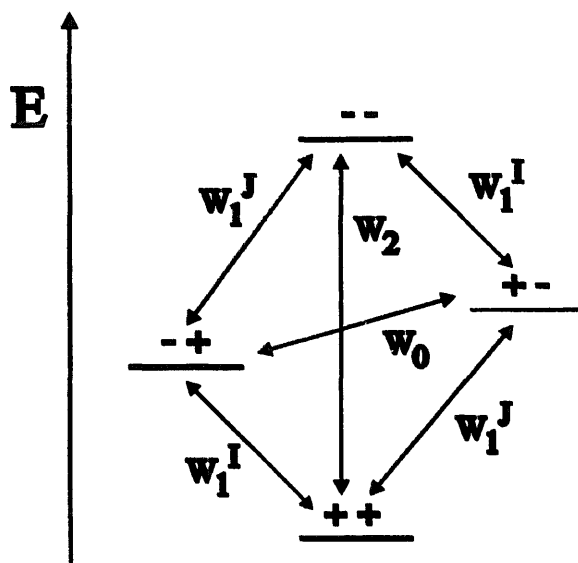


Fig. 6.1. Spin transitions and transition probabilities in a two unlike spin system experiencing dipolar coupling. The + and – refer to the signs of M_I and M_J for the two nuclear spins. The two nuclei are assumed to have positive gyromagnetic ratios.

an upper limit for its intensity, and therefore a lower limit for the efficiency of the dipolar coupling between the proton of the saturated signal and any other proton nearby.

Since the NOE is a measure of magnetization transfer between dipole-coupled nuclei, it depends on the square of the magnitude of each nuclear magnetic moment; therefore its application is essentially limited to proton NMR. In protein NMR the ^{15}N – ^1H NOE in peptide NH groups is measured to learn about the N–H reorientational correlation time.

In order to understand NOEs it is convenient to refer to an energy diagram of the type shown in Fig. 6.1 which shows the energies of two dipole coupled nuclei with $I = \frac{1}{2}$, $J = \frac{1}{2}$. In case the gyromagnetic ratios γ_I and γ_J are positive, as in the example, the ground state is that with $M_I = M_J = +\frac{1}{2}$, and the most excited level has $M_I = M_J = -\frac{1}{2}$. At intermediate energies there are the two levels, $M_I = -\frac{1}{2}$, $M_J = +\frac{1}{2}$, and $M_I = +\frac{1}{2}$, $M_J = -\frac{1}{2}$. The dipolar coupling energy averages to zero by rotation (Eq. (2.15)). Therefore, the energy levels of Fig. 6.1 do not depend on the extent of the spin–spin dipolar coupling. This figure is similar to Fig. 3.8(A), where the dipolar coupling between an electron spin and a nuclear spin was depicted. The NMR spectrum consists of two lines at energies $\hbar\gamma_I B_0$ and $\hbar\gamma_J B_0$. When the equilibrium population of two levels is altered by providing the proper frequency to the system, e.g. the frequency corresponding to the w_1^I transition, the population of all levels will be perturbed. Since the intensity of a signal in NMR depends on the difference in population between the involved levels, selective irradiation of one signal causes a change in the intensity in the other signal. As already defined, the fractional variation of intensity is just the NOE.

In the following sections we will go through the various classical experiments like

steady state, truncated and transient NOE, as well as ROE. The presentation has the twofold purpose of sketching (or refreshing) the basic theory to non-specialists, and of underlying the peculiar behavior of each experiment in paramagnetic systems.

6.2. Steady state NOE

The steady state NOE is the fractional variation η_I in the integrated NMR signal intensity of a nuclear spin I when another spin J is saturated and enough time is given to the system in order to let it reach a new steady state equilibrium. In order to fully understand the phenomenon it is convenient to refer first to a saturation time long in comparison with the T_1 of the signal on which NOE is going to be measured; for short irradiation times we will then deal with NOE as a function of time $\eta_I(t)$. We now express the intensity of a signal from spin I as the magnetization M_z^I along z , as already defined. The larger the difference in population between the M_I levels, the larger the intensity of the signal and the larger M_z^I . After saturating signal J with a proper soft pulse, we have made the population of the $++$ level equal to that of the $+-$ level, as well as that of the $-+$ level equal to that of the $--$ level (Fig. 6.1). If the saturation lasts for a long enough time (see above), the difference in population between $++$ and $-+$ levels, and between the $+-$ and $--$ levels, reaches a steady state condition and $M_z^I(t)$ reaches a new value that is different from the original equilibrium value $M_z^I(\infty)$. The NOE $\eta_{I(J)}$ (which indicates that NOE is observed on signal I when J is saturated), will be given by

$$\eta_{I(J)} = \frac{M_z^I(t) - M_z^I(\infty)}{M_z^I(\infty)} \quad (6.1)$$

It can be shown (see Appendix IV) that the following relationship holds:

$$M_z^I(t) = M_z^I(\infty) + [\sigma_{I(J)}/\rho_{I(J)}] M_z^J(\infty) \quad (6.2)$$

In order to define $\sigma_{I(J)}$ and $\rho_{I(J)}$ it is convenient to refer to Fig. 6.1 and to define w_1^I and w_1^J as the transition probabilities between two states involving a single quantum transition either of spin I or J ; w_0 is the zero quantum transition and corresponds to the $-+ \rightarrow +-$ transition and vice versa; w_2 corresponds to the $-- \rightarrow ++$ transition and vice versa, which is a double quantum transition. $\rho_{I(J)}$ is defined as

$$\rho_{I(J)} = w_0 + 2w_1^I + w_2 \quad (6.3)$$

It represents the total probability for nucleus I to change its spin component along z in a coupled two spin system.

$\sigma_{I(J)}$ ($= \sigma_{J(I)}$ when I and J have the same spin multiplicity) is called cross-relaxation rate, and is given by

$$\sigma_{I(J)} = \sigma_{J(I)} = w_2 - w_0 \quad (6.4)$$

The transitions corresponding to w_2 and w_0 involve simultaneous changes in spin

state of both nuclei. The difference between w_2 and w_0 tells us how the variation in population of J affects the equilibrium of I . In other words, one can think in terms of magnetization transfer from J to I when J is saturated. The larger the cross relaxation, the larger the dipolar coupling. The NOE on I is proportional to the cross relaxation from J and inversely proportional to the capability of I to return to equilibrium once its equilibrium is perturbed through cross relaxation.

The transition probabilities depend on the mean squared interaction energy relative to the mechanism which causes the transition, times the value of the spectral density at the required frequencies. The square of the dipolar interaction energy is, as usual, proportional to $\langle \mu_1 \cdot \mu_2 / r^3 \rangle^2$, where μ_1 and μ_2 are the magnetic moments of the two spins. The actual equations are

$$\rho_{I(J)} = \left(\frac{\mu_0}{4\pi} \right)^2 \frac{2\hbar^2 \gamma_I^2 \gamma_J^2 J(J+1)}{15r_{IJ}^6} \left[\frac{\tau_c}{1 + (\omega_I - \omega_J)^2 \tau_c^2} + \frac{3\tau_c}{1 + \omega_I^2 \tau_c^2} + \frac{6\tau_c}{1 + (\omega_I + \omega_J)^2 \tau_c^2} \right] \quad (6.5)$$

and

$$\sigma_{I(J)} = \left(\frac{\mu_0}{4\pi} \right)^2 \frac{2\hbar^2 \gamma_I^2 \gamma_J^2 J(J+1)}{15r_{IJ}^6} \left[\frac{6\tau_c}{1 + (\omega_I + \omega_J)^2 \tau_c^2} - \frac{\tau_c}{1 + (\omega_I - \omega_J)^2 \tau_c^2} \right] \quad (6.6)$$

The correlation time is the reorientational correlation time. This is generally the rotational correlation time unless internal motions of a group in a molecule are faster. In the latter case, pairs of nuclei in the same molecule can have different reorientational correlation times.

Note the analogy between Eq. (6.5) and Eq. (3.12): indeed, $\rho_{I(J)}$ is a longitudinal relaxation time of spin I due to the interaction with spin J upon reciprocal reorientation. The point is that it cannot be measured, except approximately, through a T_1 measurement because T_1 is defined in the absence of links with other nuclear spins, i.e. in the absence of cross relaxation (see Section 6.2.2).

By combining Eqs. (6.1) and (6.2), we obtain

$$\eta_{I(J)} = [\sigma_{I(J)} / \rho_{I(J)}] M_z^I(\infty) / M_z^J(\infty) \quad (6.7)$$

Since $M_z^I(\infty)$ is proportional to $I(I+1)\gamma_I$, and $M_z^J(\infty)$ is proportional to $J(J+1)\gamma_J$, in the general case of heteronuclear spins we have

$$\eta_{I(J)} = [\sigma_{I(J)} / \rho_{I(J)}] J(J+1)\gamma_J / I(I+1)\gamma_I \quad (6.8)$$

The relative values of I , J , γ_I , γ_J are important for determining the size and the sign of heteronuclear NOE; obviously, in homonuclear NOE they cancel each other and Eq. (6.7) takes the simple form

$$\eta_{I(J)} = \frac{\sigma_{I(J)}}{\rho_{I(J)}} \quad (6.9)$$

Cross relaxation can occur in principle also between nuclei coupled by a time-dependent scalar interaction. In this case only w_0 can contribute to it. The correlation time for the reorientation is either chemical exchange or the relaxation rate of nucleus J if nucleus I is observed. The correlation time is generally too long to make the experiment successful.

6.2.1. Steady state NOE in real life

The first consideration by looking at Eqs. (6.5), (6.6) and (6.7) is that NOE does not contain any structural information within the present scheme. Indeed, both $\rho_{I(J)}$ and $\sigma_{I(J)}$ contain the same r_{IJ} parameter which cancels out in $\eta_{I(J)}$. In practice, the two-spins scheme is never a good description of any real system. The nucleus I , on which NOE is going to be observed, is always coupled to other nuclei. When dealing with hyperfine coupled nuclei, often the major source of relaxation is not the coupling with J but the coupling with the unpaired electrons. The expression for $\eta_{I(J)}$ then is (Appendix IV)

$$\eta_{I(J)} = \frac{\sigma_{I(J)}}{\rho_{I(J)} + \rho_{I(\text{other})} + R_{1M}^I} = \frac{\sigma_{I(J)}}{\rho_I} \quad (6.10)$$

where $\rho_{I(J)}$, as defined above, is the contribution to longitudinal relaxation of nucleus I due to the coupling with nucleus J , $\rho_{I(\text{other})}$ includes all the couplings with other nuclei responsible for relaxation of nucleus I with the exception of the coupling with nucleus J , and R_{1M}^I is the paramagnetic contribution to the longitudinal relaxation rate of nucleus I arising from the various mechanisms described in Chapter 3. The sum of all these relaxation rates is the total rate ρ_I . Even if not important in principle, it is important in practice to underline that ρ_I is not a time constant for an exponential process; the process would be exponential only in the absence of cross relaxation. In paramagnetic compounds the total relaxation may be dominated by R_{1M}^I and the total time dependence approaches an exponential behavior [6]. Therefore, ρ_I is the measured T_1^{-1} of the nucleus (either from a selective or a non-selective experiment). When R_{1M}^I is not dominating, after a selective excitation of I , the initial return to equilibrium can be assumed to be exponential and its rate constant, $T_{1\text{sel}}^{-1}$, can be taken as ρ_I (see Section 6.2.2).

Of course, the larger the denominator in Eq. (6.10), the smaller the NOE. That is why NOE in paramagnetic complexes has developed so late: the coupling with unpaired electrons makes the relaxation very effective and the NOE very small. In geminal protons belonging to macromolecules ($\tau_r \approx 10^{-8}$ s) with ρ_I of, say, 100 s^{-1} due to paramagnetic contributions, the NOE is about 20% at 500 MHz. If the distance between protons increases to 3 Å the NOE drops to 0.8%. In small complexes τ_r is typically 10–100 times shorter than in the above example and the NOEs have intensities smaller by a similar amount. The problem would be hopeless if we could not gain one to two orders of magnitude in sample concentration. It is therefore important to have a strict control of the temperature (remember that the hyperfine shift is temperature dependent) during the hours of summation of the difference

FIDs (see Section 9.3), and to increase the signal to noise ratio until 1% differences can be measured with a precision of two figures.

When the denominator in Eq. (6.10) is dominated by the paramagnetic contribution to nuclear relaxation ($\rho_I \simeq R_{1M}^I$), the following simplified equation holds

$$\eta_{I(J)} = \sigma_{I(J)} / R_{1M}^I = \sigma_{I(J)} T_{1M}^I \quad (6.11)$$

In Eq. (6.11) the r^{-6} parameter is not canceled out, because $\sigma_{I(J)}$ depends on r_{IJ}^{-6} but R_{1M}^I does not. When the nucleus–electron coupling is dipolar in origin, R_{1M}^I depends on r^{-6} where r is the distance between the resonating nucleus and the unpaired electron (Eq. (3.16)).

When measuring steady state NOE, the effect measured on saturating I or on saturating J may be different because ρ_I and ρ_J are in general different. We say that steady state NOE is not symmetric. It follows that larger NOEs, and then more favorable cases, occur when the signal with larger ρ is saturated.

6.2.2. Selective and non-selective T_1

It is intuitive that the NOE will be larger the larger the cross relaxation, and smaller the larger ρ_I . It may be appropriate here to discuss in a more quantitative way the response of a dipole-coupled two spin system to selective and non-selective experiments, and the relationship between the results of these experiments and the quantity of interest, ρ_I . The qualitative behavior has been anticipated in Section 3.13. As already described (and see also Section 9.2), when measuring T_1 of a signal one can excite (for instance, invert) all the signals simultaneously (non-selective experiment). If the nuclei are dipole coupled, then they will return to equilibrium also by exchanging magnetization through cross relaxation. Alternatively, only one signal is inverted (selective experiment) and its return to equilibrium measured. Cross relaxation will be different from the previous case. In both cases, the return to equilibrium is not exponential in the presence of cross relaxation. If this is the case, the measurement of T_1 is approximate, and even the definition of T_1 may be invalid. This is because the other nuclei are part of the lattice but this lattice does not possess the infinite heat capacity required to have an exponential behavior of the magnetization. In fact, cross relaxation is capable of affecting the spin state populations of the other nuclei.

We start from the expression for dM_z^I/dt derived in Appendix IV (Eq. (IV.13)) and write the corresponding expression for dM_z^J/dt :

$$\begin{aligned} \frac{dM_z^I(t)}{dt} &= -[M_z^I(t) - M_z^I(\infty)]\rho_I - [M_z^J(t) - M_z^J(\infty)]\sigma_{I(J)} \\ \frac{dM_z^J(t)}{dt} &= -[M_z^J(t) - M_z^J(\infty)]\rho_J - [M_z^I(t) - M_z^I(\infty)]\sigma_{I(J)} \end{aligned} \quad (6.12)$$

where we have substituted $\rho_{I(J)}$ and $\sigma_{I(J)}$ with the corresponding total rates ρ_I and

ρ_J (Eq. (6.10)). The two equations, analogous to those encountered in the case of chemical exchange (Section 4.3.4), constitute a system of coupled differential equations which are relevant also for the transient experiments discussed in Sections 6.4 and 6.5, and whose general solutions are

$$\begin{aligned} M_z^I(t) &= M_z^I(\infty) + C_1 \exp(-\lambda_1 t) + C_2 \exp(-\lambda_2 t) \\ M_z^J(t) &= M_z^J(\infty) + \frac{\lambda_1 - \rho_I}{\sigma_{J(I)}} C_1 \exp(-\lambda_1 t) + \frac{\lambda_2 - \rho_I}{\sigma_{J(I)}} C_2 \exp(-\lambda_2 t) \end{aligned} \quad (6.13)$$

where $\lambda_{1,2} = \rho \pm D$, and

$$\rho = \frac{1}{2}(\rho_I + \rho_J) \quad D = \frac{1}{2}[(\rho_I - \rho_J)^2 + 4\sigma_{I(J)}\sigma_{J(I)}]^{1/2} \quad (6.14)$$

The explicit expressions for C_1 and C_2 can be derived for many particular cases [3], including the selective and non-selective inversion recovery experiments of interest here. For the selective case

$$C_1 = \frac{2(\lambda_2 - \rho_I)M_z^I(\infty)}{\lambda_1 - \lambda_2} \quad C_2 = -\frac{2(\lambda_1 - \rho_I)M_z^I(\infty)}{\lambda_1 - \lambda_2} \quad (6.15)$$

and, for the non-selective experiment

$$\begin{aligned} C_1 &= 2M_z^I(\infty) \frac{\lambda_2 - \rho_I}{\lambda_1 - \lambda_2} - 2M_z^J(\infty) \frac{\sigma_{J(I)}}{\lambda_1 - \lambda_2} \\ C_2 &= -2M_z^I(\infty) \frac{\lambda_1 - \rho_I}{\lambda_1 - \lambda_2} + 2M_z^J(\infty) \frac{\sigma_{J(I)}}{\lambda_1 - \lambda_2} \end{aligned} \quad (6.16)$$

Calculated magnetization recovery profiles are reported in Fig. 3.16. It is clear that in no case is the recovery exponential. However, Eq. (6.13) for $M_z^I(t)$ can be approximated to a single exponential, not only when $|\sigma_{J(I)}| \ll |\rho_I - \rho_J|$, as is obvious, but also when, on the contrary, $|\sigma_{J(I)}| \gg |\rho_I - \rho_J|$. In these cases, fitting the recovery to an exponential gives a rate constant close to ρ_I [6]. In contrast, in the non-selective experiment, the recovery is closer to $\rho_I + \sigma_{J(I)}$. In order to estimate ρ_I from T_1 -type measurements, the best way is that of performing a selective experiment and to measure the variation of magnetization during an initial short time. Under these circumstances the system maximizes the two contributions to the measured ρ_I (i.e. $\rho_{I(J)}$ and $\rho_{I(\text{other})}$), R_{1M}^I remaining independent of the duration of the measurement. However, in order to extract structural information through, e.g. Eq. (3.16), it is more appropriate to perform non-selective experiments. This is particularly true in the slow motion limit, where $\sigma_{I(J)} \rightarrow -\rho_{I(J)}$. Under these conditions, and neglecting $\rho_{I(\text{other})}$, $\rho_I + \sigma_{I(J)} \rightarrow R_{1M}^I$. This can be intuitively understood because cross relaxation in a non-selective experiment contributes less to signal recovery, especially at the beginning of the experiment, and the latter is dominated by paramagnetic effects (R_{1M}^I). In any case, when ρ_I in paramagnetic systems is very large (e.g. 100–1000 s⁻¹),

it means that R_{1M}^I dominates the relaxation processes and the results of selective and non-selective experiments are close to one another¹.

6.2.3. Steady state NOE in paramagnetic compounds

By combining Eqs. (6.5) and (6.6) we realize that there is an NOE dependence on the magnetic field and on the reorientational correlation time. In Fig. 6.2(A) the NOE dependence on the external magnetic field is shown for τ_r of 10 ns and for two protons at 1.8 Å, by taking $\rho_{I(\text{other})} = 0$ and $R_{1M}^I = 0, 50$ and 200 s^{-1} . The dependence on τ_r under the same conditions is shown at 300 MHz (Fig. 6.2(B)). From Fig. 6.2(A) it appears that at low $\omega\tau$ values (fast motion limit) the maximal homonuclear NOE is 0.5, whereas at large values of $\omega\tau$ (slow motion limit) the maximal NOE is -1 . Of course, these are limiting values in the absence of R_{1M}^I (and $\rho_{I(\text{other})}$): the hyperfine coupled relaxation decreases the above absolute values, but leaves the dependence unaltered. The NOE is larger at larger magnetic fields and/or when rotation is slowed down (Fig. 6.2(B)). It is important to note that, for very long τ_r values, NOE values close to -1 could in principle be achieved even in the presence of paramagnetic relaxation; this is because $\sigma_{I(I)}$ increases with τ_r , whereas the denominator of Eq. (6.10) increases less because R_{1M}^I does not depend on τ_r , but rather on τ_s . Sometimes, with small proteins, it is even convenient to add ethylene glycol to their water solutions in order to increase viscosity and then τ_r . In the literature this has been done for met-myoglobin [7] and for Co₇thioneins [8].

Steady state NOEs in paramagnetic small complexes under the conditions of fast rotation ($MW < 800\text{--}2500$ Da depending on the magnetic field) are small and sometimes may be below detection. In Table 6.1 the steady state NOE intensities are reported for various τ_r values (and the corresponding molecular weight values estimated from the Stokes–Einstein relation (Eq. (3.7)) and for various R_{1M}^I values. For each pair of τ_r and R_{1M}^I values the NOE intensities are calculated for distances of 1.8 and 3.0 Å and for magnetic fields of 200 and 600 MHz. From inspection of the table it appears that NOE measurements on small complexes may be successful for high concentrations at low magnetic fields, or at large magnetic fields when rotation is slowed down by using viscous solvents or mixtures of solvents. On the contrary, macromolecules seem perfectly suited for this type of experiment since they fall in the slow motion regime.

In Table 6.2 some significant examples of the NOEs observed in the paramagnetic systems investigated up to now are reported [9]; as expected, as the T_1 values

¹ Note added in proof. Cross relaxation is the main cause of deviation from exponentiality, both for diamagnetic and paramagnetic non-selective relaxation recovery. However, a non-selective inversion recovery can be pragmatically interpreted on the basis of a single exponential. The problem arises of whether the extracted R_{1M}^I can be used, according to the Solomon equation, to extract metal-proton distances. Though this problem has been stressed in a negative sense (G.N. La Mar and J.S. de Ropp, in L.J. Berliner and J. Reuben (Eds.), *Biological Magnetic Resonance*, Plenum, New York, Vol. 12, 1993), we optimistically advise (I. Bertini, C. Luchinat and A. Rosato, *Progr. Biophys. Mol. Biol.*, in press) (i) to check exponentiality; (ii) to extract distance parameters, with the only caution regarding geminal protons (having large cross relaxation) whose distances from the metal, however, cannot differ much.

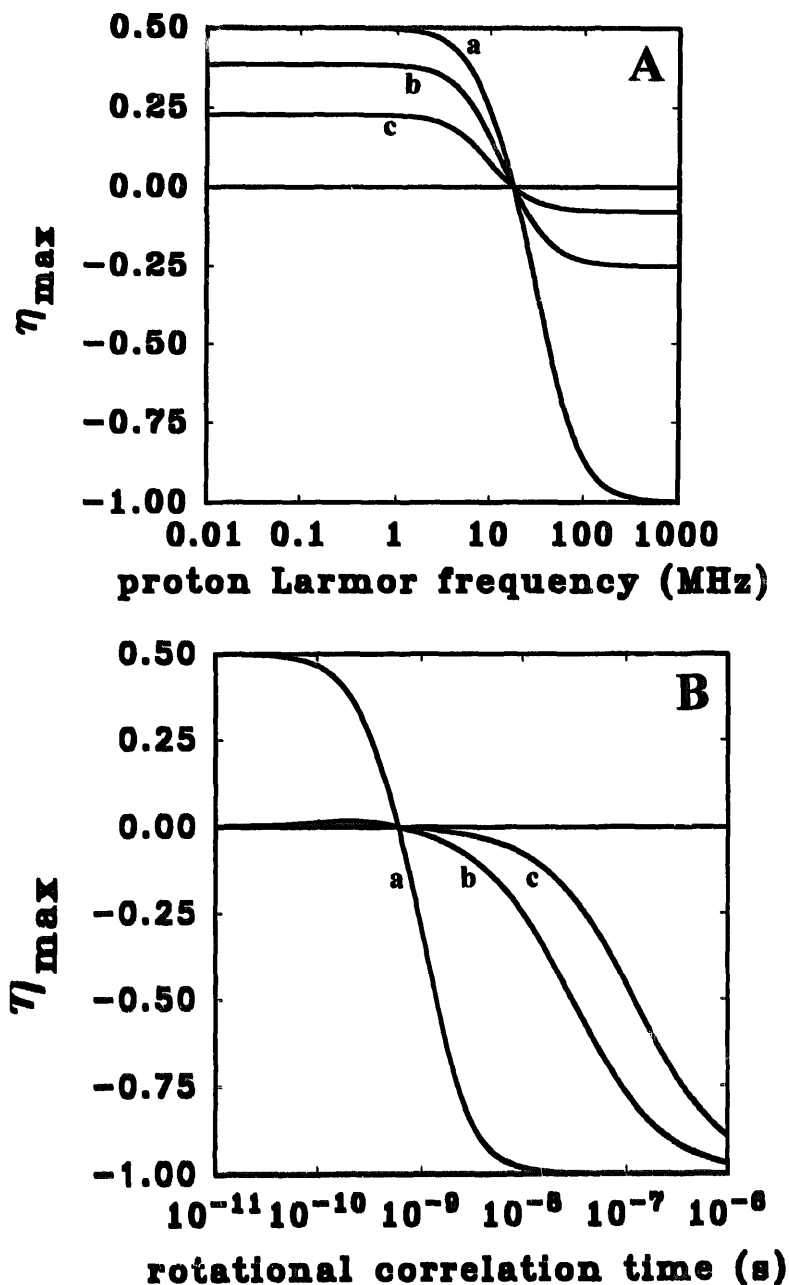


Fig. 6.2. NOE values as a function of (A) magnetic field for $\tau_r = 10$ ns and (B) τ_r at a field of 300 MHz, for two hydrogen nuclei at 1.8 Å distance ($\rho_{H(J)} = 23.6 \text{ s}^{-1}$ in the fast motion and 2.36 s^{-1} in the slow motion regime). Curves (a), (b) and (c) refer to a field-independent $R_{1M}^I = 0, 50$ and 200 s^{-1} respectively.

become shorter, the NOE drops to small values, which can be difficult to “extract” from the noise. However, the NOE increases as the molecular size increases. In Fig. 6.3 the NOEs for a protein of MW 10000 containing the cluster $\text{Fe}_4\text{S}_4^{3+}$ are shown when the hyperfine shifted signals due to coordinated β cysteine protons and lying outside the -20 – 20 ppm spectral window are saturated [10]. The NOE difference spectra show many connectivities with other signals which belong to

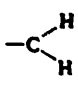
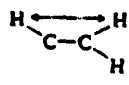
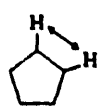
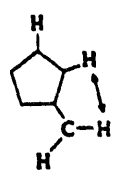
Table 6.1

Calculated steady state NOEs (%) for various values of τ , and R_{1M}' . For each τ , and R_{1M}' value two NOEs are calculated for interproton distances of 1.8 and 3.0 Å and for nuclear Larmor frequencies ν_0 of 200 and 600 MHz

τ (s)	r_{ij} (Å)	R_{1M}' (s ⁻¹)	2		4		8		16		32		64		128		256	
			ν_0 (MHz)		ν_0 (MHz)		ν_0 (MHz)		ν_0 (MHz)		ν_0 (MHz)		ν_0 (MHz)		ν_0 (MHz)		ν_0 (MHz)	
			200	600	200	600	200	600	200	600	200	600	200	600	200	600	200	600
10^{-11}	1.8	7.171	7.132	3.862	3.840	2.009	1.997	1.025	1.019	0.518	0.515	0.260	0.259	0.130	0.130	0.065	0.033	0.032
[25]	3.0	0.388	0.385	0.195	0.193	0.097	0.097	0.049	0.049	0.024	0.024	0.012	0.012	0.006	0.006	0.003	0.002	0.002
$10^{-10.5}$	1.8	17.221	16.476	10.466	9.897	5.808	5.502	3.064	2.914	1.591	1.502	0.808	0.762	0.407	0.384	0.205	0.193	0.192
[80]	3.0	1.197	1.130	0.606	0.571	0.305	0.287	0.153	0.144	0.077	0.072	0.038	0.036	0.019	0.018	0.010	0.009	0.005
10^{-10}	1.8	30.088	22.236	21.697	15.130	13.929	9.230	8.117	5.186	4.424	2.764	2.317	1.429	1.186	0.727	0.600	0.367	0.302
[250]	3.0	3.380	2.098	1.750	1.076	0.891	0.545	0.450	0.274	0.26	0.138	0.113	0.069	0.057	0.034	0.028	0.017	0.014
$10^{-9.5}$	1.8	31.860	2.420	26.017	1.674	19.035	1.035	12.387	0.587	7.293	0.315	4.001	0.163	2.103	0.083	1.079	0.042	0.547
[800]	3.0	0.700	0.239	3.063	0.123	1.591	0.062	0.811	0.031	0.410	0.016	0.206	0.008	0.103	0.004	0.052	0.002	0.001
10^{-9}	1.8	6.365	51.146	5.256	38.153	3.897	25.299	2.569	15.114	1.528	8.373	0.844	4.425	0.445	2.278	0.229	1.156	0.582
[2500]	3.0	1.198	6.426	0.647	3.352	0.337	1.713	0.172	0.866	0.087	0.435	0.044	0.218	0.022	0.109	0.011	0.005	0.027
$10^{-8.5}$	1.8	68.209	82.145	59.727	71.018	47.832	55.879	34.206	39.177	21.791	24.519	12.626	14.025	6.858	7.556	3.583	3.931	2.006
[8000]	3.0	17.482	19.551	9.821	10.866	5.234	5.754	2.706	2.965	1.376	1.505	0.694	0.758	0.349	0.381	0.175	0.191	0.095
10^{-8}	1.8	92.235	94.128	87.379	89.116	79.055	80.540	66.403	67.541	50.302	51.058	33.875	34.312	20.491	20.720	11.447	11.561	6.136
[25000]	3.0	43.190	43.799	27.726	28.061	16.156	16.327	8.806	8.891	4.611	4.653	2.361	2.382	1.195	1.205	0.601	0.606	0.304
$10^{-7.5}$	1.8	97.918	98.122	96.139	96.338	92.770	92.957	86.693	86.861	76.650	76.790	62.232	62.334	45.221	45.285	29.236	29.272	17.146
[80000]	3.0	71.060	71.184	55.183	55.268	38.140	38.190	23.576	23.603	13.368	13.381	7.164	7.171	3.715	3.719	1.893	1.895	0.956
10^{-7}	1.8	99.383	99.404	98.797	98.818	97.646	97.666	95.421	95.441	91.263	91.281	83.947	83.963	72.347	72.360	56.682	56.691	39.559
[250000]	3.0	88.639	88.657	79.612	79.627	66.140	66.151	49.415	49.422	32.818	32.822	19.631	19.633	10.884	10.885	5.755	5.756	2.963

Table 6.2

Some examples of NOE detected on paramagnetically shifted signals in metalloproteins [9]

Group ^a	H–H distance (Å)	NOE ^b (%)	T_1 (ms)	MW	τ_r (ns)
 (Asp, Glu, Cys, His)	1.8	6	8.4	9000	4
		5	3.6	11000	5
		7	5.6	11000	5
		43	120	16000	9
		7.7	2.4	32000	14
		60	100	36000	21
 (Cys)	2.2–2.4	4.5	34.0	9000	4
		1.8	5.6	11000	5
 (His)	2.4	6	5.4	30000	14
		0.9	1.8	32000	14
		2	4.2	32000	14
 (His)	~ 3.3	0.6	3.5	32000	14
		7–10	—	42000	21

^a The groups bearing the two protons belong to metal ion ligands. ^b The NOEs in the present systems are all negative; they are reported here without the minus sign.

nearby groups, as well as strong connectivities with the respective geminal protons (not shown).

The difference spectra in Fig. 6.3 also show signals (marked with \times) arising from saturation transfer to another species in chemical exchange. Indeed, the experiment for detecting steady state NOE is absolutely identical to that used to detect magnetization transfer in the presence of chemical exchange (Section 4.3.4). Therefore, it is not possible to distinguish, from the experimental point of view, real NOE from chemical exchange effects in the limit of slow motion. Actually, the values of NOE are always a fraction of the signal intensity, which in paramagnetic molecules is often small (of the order of 1%), whereas saturation transfer can change the intensity of the signal really up to 100% even in paramagnetic molecules.

In diamagnetic compounds we face the problem that after saturation of signal J the Zeeman population of nuclei I may be largely affected, and this may cause further magnetization transfer on other nuclei to which nucleus I is coupled. Such

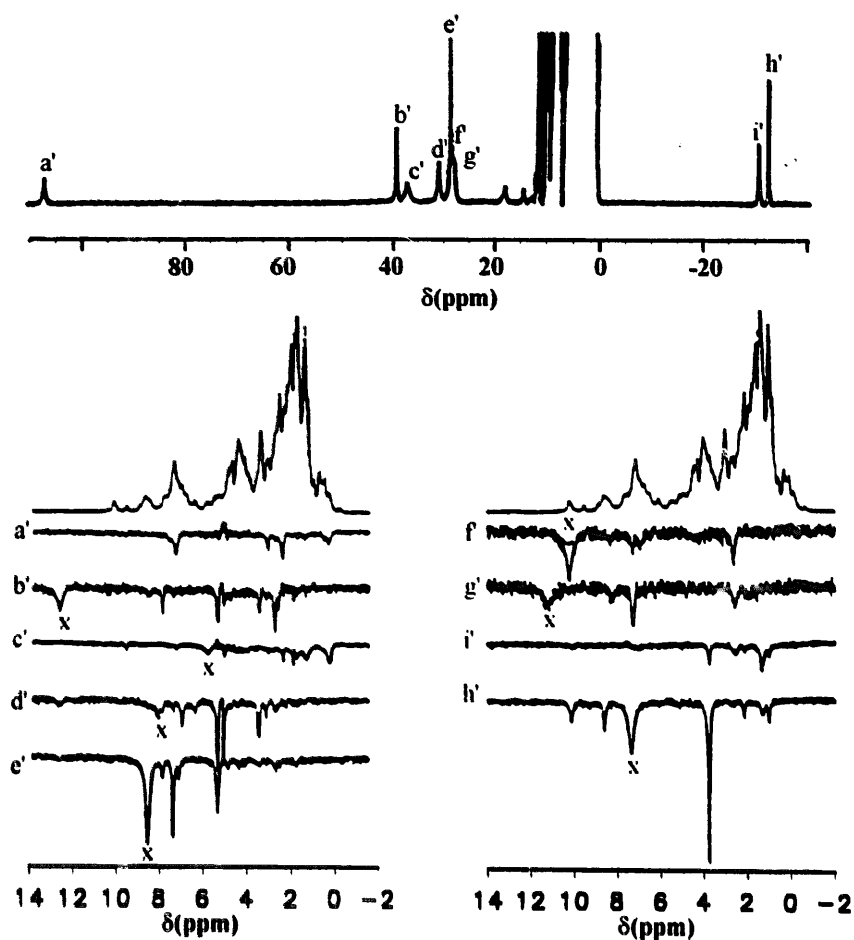


Fig. 6.3. NOE difference spectra obtained upon saturation of the hyperfine shifted signals corresponding to the β -CH₂ protons of the Fe₄S₄-coordinated cysteines in oxidized HiPIP from *C. vinosum* [10]. Signals marked by \times arise from saturation transfer to a small amount of reduced species [10].

coupling indeed accounts for the $\rho_{I(\text{other})}$ term in Eq. (6.10). It follows that a secondary NOE can be observed on signal K not because J is coupled with K but because I is coupled with K . This phenomenon is called spin diffusion. It is not relevant in the fast motion limit, because the NOEs are usually small and, therefore, the smaller is the secondary magnetization transfer to nearby nuclei; furthermore, and more importantly, a positive sign of σ means that a decrease in M_z^J causes an *increase* in M_z^I which, in turn, causes a *decrease* in M_z^K , and so on. This alternation in sign eventually results in substantial cancellation of the long range effects, because a nucleus very far from the saturated nucleus will experience both positive and negative contributions depending on whether the number of intermediate spins on the various cross relaxation pathways is even or odd.

In contrast, sizable spin diffusion may be operative in the slow motion regime. Of course, this phenomenon may terribly complicate the analysis of NOEs, until they become useless. After saturating one signal, many or even all signals of the molecule may be affected in a cascade fashion. However, in paramagnetic macromolecular

systems the major source of relaxation for signal *I* can be the coupling with the unpaired electrons; so it returns to equilibrium prior to appreciably transferring magnetization to nucleus *K*. Therefore, spin diffusion effects are limited. The counterpart of this simplification is that the NOE is dramatically reduced by the short ρ_I values.

An example is available in the literature where the spin diffusion effects are evaluated in a paramagnetic system [11]. It is the $\text{Cu}_2\text{Co}_2\text{SOD}$ discussed in Section 5.3.3. The scheme is again reported here (Fig. 6.4 with its labeling) for convenience. In Table 6.3 the NOEs at 200 MHz on all the proton ligands are reported when they are saturated one after the other. The T_1 values measured at the same field are also reported [12,13]. The interproton distances are known from the X-ray structure and the value of the reorientational correlation time estimated by the Stokes–Einstein equation (Eq. (3.7)). The NOEs calculated through the two-spin approximation are in satisfactory agreement with the experimental NOEs. If then a

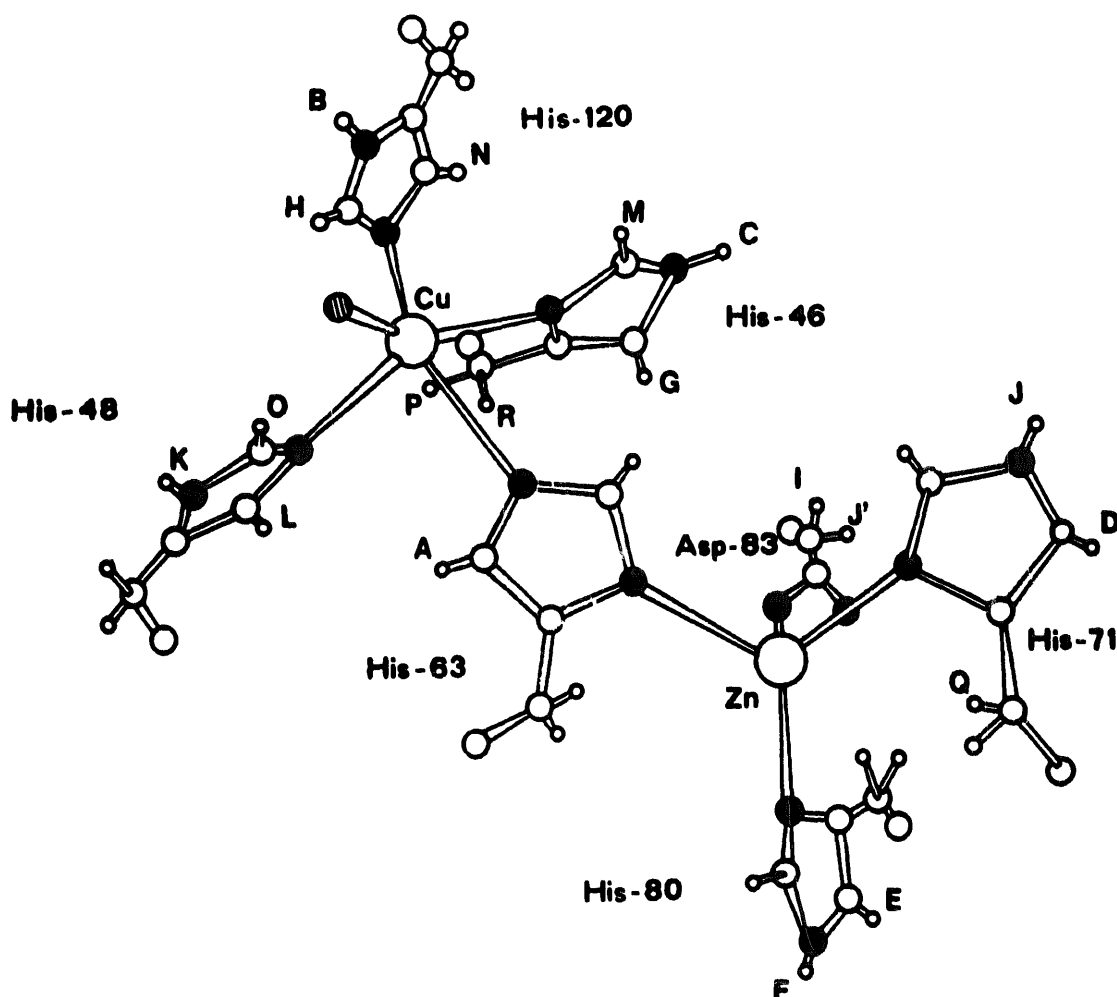


Table 6.3

Non-selective T_1 and NOE values in bovine $\text{Cu}_2\text{Co}_2\text{SOD}$ at 200 MHz [13]. The distances calculated from the NOE values using the two-spin approximation agree with available X-ray distances

Saturated signal	Observed signal	T_1 (obs) (ms)	NOE (%)	r (calc) (Å)	r (X-ray) (Å)
A H δ 2 His 63	L H δ 2 His 48	4.3	0.9 ± 0.1	2.7 ± 0.2	2.7
A H δ 2 His 63	K H δ 1 His 48	8.0	0.6 ± 0.2	3.2 ± 0.3	3.8
A H δ 2 His 63	R H β 2 His 46	2.4	0.2 ± 0.1	3.3 ± 0.3	3.4
B H δ 1 His 120	H H ϵ 1 His 120	1.8	1.0 ± 0.2	2.3 ± 0.2	2.4
C H ϵ 2 His 46	G H δ 2 His 46	3.5	1.4 ± 0.2	2.4 ± 0.2	2.5
C H ϵ 2 His 46	M H ϵ 1 His 46	2.7	0.9 ± 0.1	2.5 ± 0.2	2.5
G H δ 2 His 46	C H ϵ 2 His 46	4.2	1.7 ± 0.4	2.4 ± 0.2	2.5
M H ϵ 1 His 46	C H ϵ 2 His 46	4.2	2.2 ± 0.2	2.4 ± 0.2	2.5
R H β 2 His 46	G H δ 2 His 46	3.5	0.6 ± 0.2	2.8 ± 0.3	3.3
Q H β 1 His 71	D H δ 2 His 71	3.8	1.4 ± 0.2	2.4 ± 0.2	2.8
L H δ 2 His 48	γ_1 CH ₃ Val 118	70.0	33.0 ± 6	2.8 ± 0.3	2.8
R H β 2 His 46	P H β 1 His 46	1.6	5.4 ± 0.8	1.7 ± 0.2	1.6
P H β 1 His 46	R H β 2 His 46	2.4	9.0 ± 1.0	1.7 ± 0.2	1.6
L H δ 2 His 48	P H β 1 His 46	1.6	1.3 ± 0.3	2.2 ± 0.2	2.3
P H β 1 His 46	L H δ 2 His 48	4.3	5.5 ± 1.0	2.0 ± 0.2	2.3
L H δ 2 His 48	R H β 2 His 46	2.4	0.5 ± 0.1	2.6 ± 0.3	3.2
R H β 2 His 46	L H δ 2 His 48	4.3	2.3 ± 0.2	2.3 ± 0.2	3.2

matrix is considered where all the ligand protons plus other protons from nearby groups are allowed to cross relax, the newly calculated NOEs are still close to the experimental values [11]. Spin diffusion is quenched by the fast relaxing nature of the system. The ρ_1 values are well above 100 s^{-1} . When the ρ_1 values are smaller, spin diffusion may occur even in paramagnetic systems; tricks are developed to detect spin diffusion and to minimize it (see the next two sections).

6.3. Truncated NOE

Up to now we have been interested in steady state NOEs, i.e. when one signal is saturated for a long time with respect to T_1 of the nucleus on which NOE is going to be measured. We are interested here in understanding what happens when the saturation time is short and variable. The resulting NOE is called truncated NOE [14] because not enough time is left for full magnetization transfer. These experiments are of fundamental importance for the measurement of ρ_1 , for evaluating cross relaxation, and to avoid or to measure spin diffusion.

In Appendix IV, where the steady state NOE has been derived, the equation for the NOE as a function of the irradiation time is also derived. In the case of homonuclear NOE, we have

$$\eta_{II}(t) = [\sigma_{II}(t)/\rho_I][1 - \exp(-\rho_I t)] \quad (6.17)$$

We can easily verify that for t long with respect to ρ_1 , the exponential term tends to

zero and we are back to the case of steady state NOE (Eq. (6.10)). For t tending to zero, the NOE tends to zero. The dependence of $\eta_{I(J)}(t)$ on t is reported in Fig. 6.5 for the same parameters as in Fig. 6.2. For times short with respect to ρ_I [$1 - \exp(-x) \approx 1 - (1 - x) = x$], we have

$$\eta_{I(J)}(t) = \sigma_{I(J)}t \quad (6.18)$$

For irradiation times of short J with respect to the relaxation time of I the NOE extent is independent of the relaxation time of the nucleus and provides a direct measurement of $\sigma_{I(J)}$. If the time required to saturate signal J is not negligible compared with t , the response of the system is not linear [15]. The truncated NOE is independent of paramagnetism as it does not depend on ρ_I , which contains the electron spin vector S in the R_{1M}^I term, and only depends on $\sigma_{I(J)}$, which does not contain S . If then the steady state NOE is reached, the value of ρ_I can also be obtained. This is the correct way to measure ρ_I of a nucleus, provided saturation of J can be considered instantaneous. In general, measurements at short t values minimize spin diffusion effects. In fact, in the presence of short saturation times, the transfer of saturation affects mainly the nuclei directly coupled to the one whose signal is saturated. Secondary NOEs have no time to build substantially. As already said, this is more true, in paramagnetic systems, the larger the R_{1M}^I contribution to ρ_I .

Measuring the build up of NOE is necessary everytime the NOE is provided by

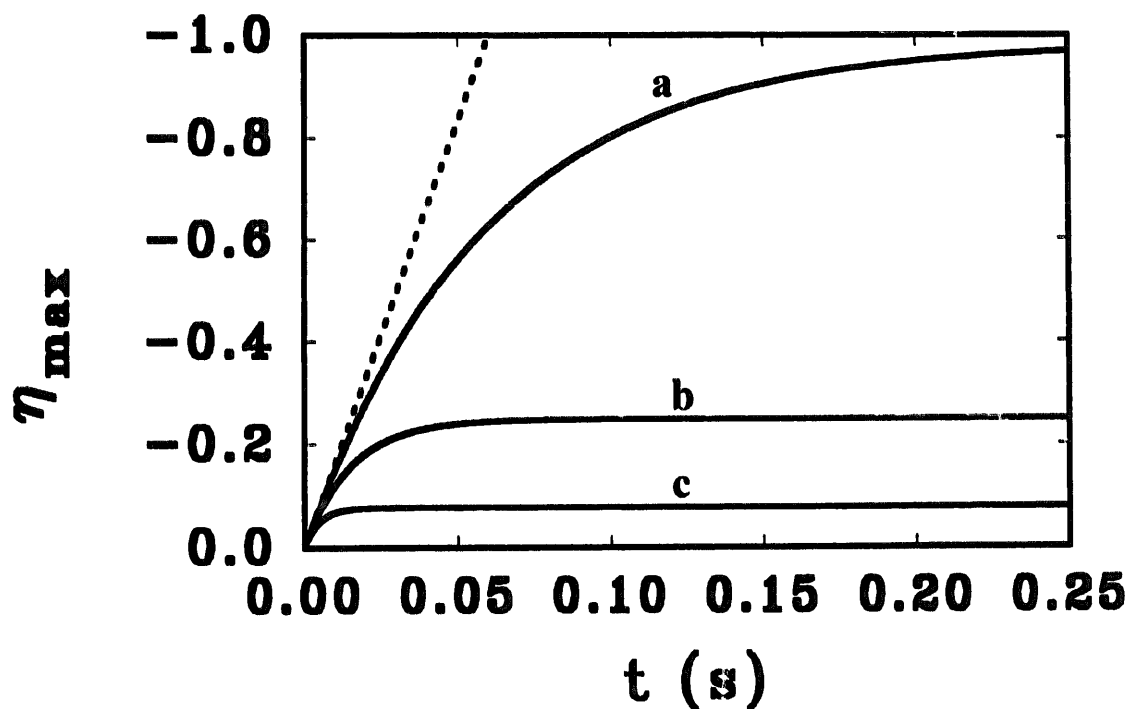


Fig. 6.5. NOE values as a function of irradiation time t , calculated according to Eqs. (6.5), (6.6) and (6.17). Conditions: $\tau_r = 10$ ns, 300 MHz, for two hydrogen nuclei 1.8 Å apart ($\rho_{I(J)} = 2.38 \text{ s}^{-1}$). $\rho_{I(\text{other})} = 0$, $R_{1M}^I = 0, 50$ and 200 s^{-1} for curves (a), (b) and (c) respectively. The initial (dashed line) is the same in all cases and equals $\sigma_{I(J)}$.

a signal buried in an envelope of many other signals. Such a procedure allows one to estimate, besides the shift, ρ_I of such buried signal. From the initial part of the slope the distance between the two nuclei can be obtained. If ρ_I is dominated by R_{1M}^I , the distance from the metal can also be guessed.

6.4. Transient NOE

The populations of the spin states can be disturbed from their equilibrium condition also by applying strong r.f. pulses at the resonance frequency of one of the spins. Typically a selective 180° pulse is used. Then the decay of the system to equilibrium is observed. This kind of experiment is called transient NOE. This experiment can be used to reduce the effects of spin diffusion. After the 180° pulse the magnetization of J is inverted. The system returns to equilibrium with its own ρ_J and through cross relaxation with I (among other nuclear spins). The difference with the steady state NOE is that the time evolution of M_z^J now also plays a role. After a delay time τ , a 90° observation pulse is applied and the FID is recorded. The magnitude of the NOE as a function of time is the result of two competing effects. One is the return to equilibrium of nucleus J which causes a decrease in the absolute value of magnetization. In fact, when J is at equilibrium, no magnetization transfer occurs any more. The larger the difference in magnetization with respect to the equilibrium magnetization, the larger is the buildup of NOE. At $t=0$ the cross relaxation contribution is twice that of a steady state experiment, since in the transient case the magnetization is inverted, whereas in the steady state case it is zero. The second competing effect is the buildup of NOE, which is of the type of Eq.(6.17). The resulting transient NOE can be obtained as a particular solution of Eq. (6.13) for $M_z^I(t)$ as [3]

$$\eta_{I(J)} = \exp[-(\rho_I - D)t][1 - \exp(-2Dt)] \quad (6.19)$$

where ρ and D have been already defined (Eq. (6.14)). It appears that the transient NOE is described by a buildup function $(1 - \exp(-2Dt))$ multiplied by a decay function $(\exp[-(\rho_I - D)t])$. The initial slope is $2D$.

In case $\rho_I = \rho_J = \rho$, $D = \sigma_{I(J)}$, and Eq. (6.19) takes the following simpler form:

$$\eta_{I(J)} = \exp[-(\rho - \sigma_{I(J)})t][1 - \exp(-2\sigma_{I(J)}t)] \quad (6.20)$$

The initial slope in this case is $2\sigma_{I(J)}$.

Note that the transient NOE effect is symmetrical, in the sense that by selective excitation of I or J the same variation in intensity of the other signal is observed, even in the case of different relaxation rates.

The buildup and decay of NOE as a function of time according to Eq. (6.20) is reported in Fig. 6.6. In transient experiments, J is selectively inverted in a time assumed negligible with respect to that necessary for the NOE to build up on I . During the buildup, J also relaxes, and therefore the effect on I will depend on ρ_J , in addition to ρ_I and $\sigma_{I(J)}$. If J is relaxing much faster than I , after selective excitation

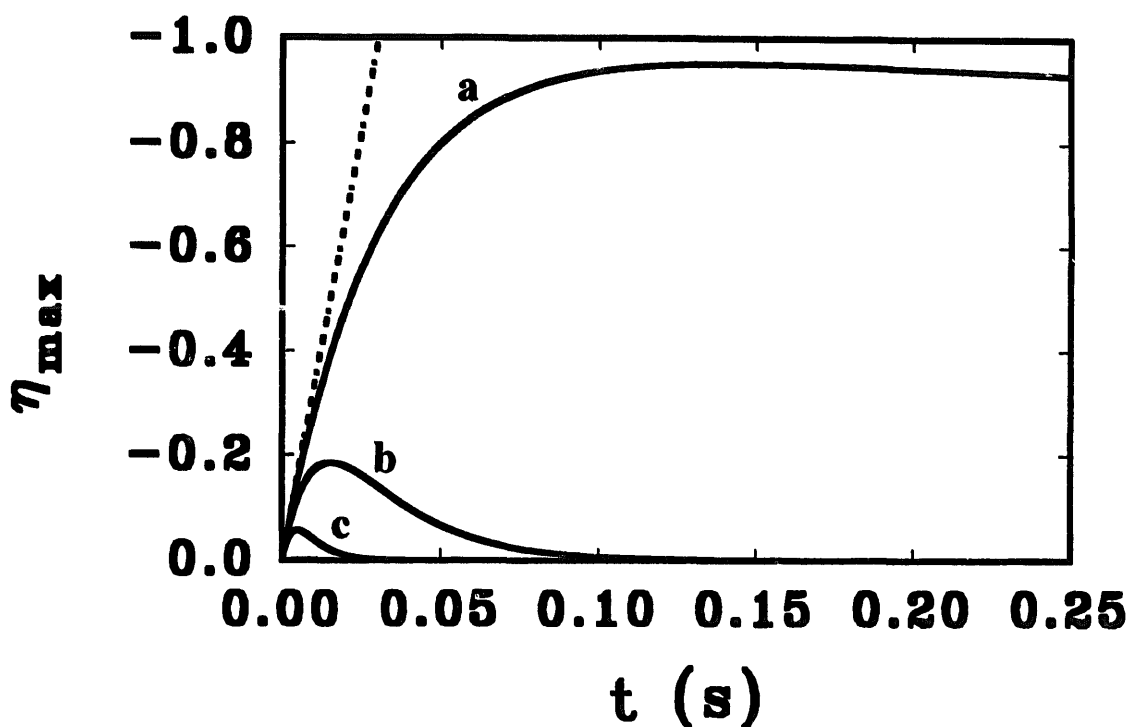


Fig. 6.6. NOE values as a function of time t in transient NOE experiments, calculated according to Eqs. (6.5), (6.6) and (6.20). The parameters are the same as in Fig. 6.5.

of J NOE starts to buildup on I but, as J relaxes efficiently, NOE starts to decrease with $\rho \approx \rho_J/2$ according to Eq. (6.14). If, however, the slow relaxing spin I is selectively excited, NOE on the fast relaxing spin J develops, but the effect soon ceases owing to the relaxation of J itself. Therefore, the effect is symmetrical. When nuclear relaxation times are short, as may happen in paramagnetic systems, the transient NOE rapidly drops to zero. This is clearly shown in Fig. 6.6, where for R'_{1M} of the order of 200 s^{-1} the transient NOE develops to a small fraction of when R'_{1M} is 50 s^{-1} , and rapidly disappears with time.

In this type of experiment the NOE buildup tends to disappear with ρ_I . In the steady state case, the saturation time is always long enough to allow spin I to cross-relax with other spins, even if ρ_I is large. In transient experiments, the cross relaxation with spin I is by itself limited in time and, ρ_I being the same, cross relaxation with other spins is drastically limited. In any case, spin diffusion is limited in that region of time in which NOE is growing (Fig. 6.6). Truncated and transient NOEs performed with short NOE buildup times are efficient in quenching spin diffusion.

One important matter is the extent of NOE in the transient and steady state cases. In the case of diamagnetic molecules the former is superior because it reduces spin diffusion and has a maximum value at $t = T_1$ (for the limit case of I and J equally relaxing). In paramagnetic systems the working conditions are much more severe for at least two reasons. One is that the time at which the maximum transient NOE is developed is very short and it may be difficult to set the exact value of the parameter. The second is that a 180° pulse has to occur in a time short with respect

to the reciprocal of the average of the longitudinal and transverse relaxation rates of J , $1/2(\rho_{1J} + \rho_{2J})^{-1}$. In order to meet this condition a high power pulse may be needed. Of course, a high power pulse for a short time is hardly selective, and artifacts in the experiment are often encountered. In Fig. 6.7, the calculated time dependence of transient and truncated NOE is reported. A larger NOE is observed in the transient case only in a narrow range of time. In the authors' experience, a steady state or truncated NOE is much safer!

The limiting values of η are 0.385 and -1 in the fast and slow motion limits respectively (Fig. 6.8). In other words, the steady state NOE is a more sensitive technique for small molecules (0.5 vs. 0.385).

6.5. NOE in the rotating frame (ROE)

Rotating frame NOE experiments, ROE [16], measure the transfer of transverse magnetization, spin locked in the transverse plane, within a pair of spins. The pulse sequence consists of a selective 180° pulse on J , followed by a non-selective 90° pulse. At this point, J is along $-y$ and I is along y (Fig. 6.9). During a time t before acquisition, a spin locking r.f. is applied, in such a way that the B_1 field is parallel to the initial magnetization along y in the rotating frame. Magnetization transfer

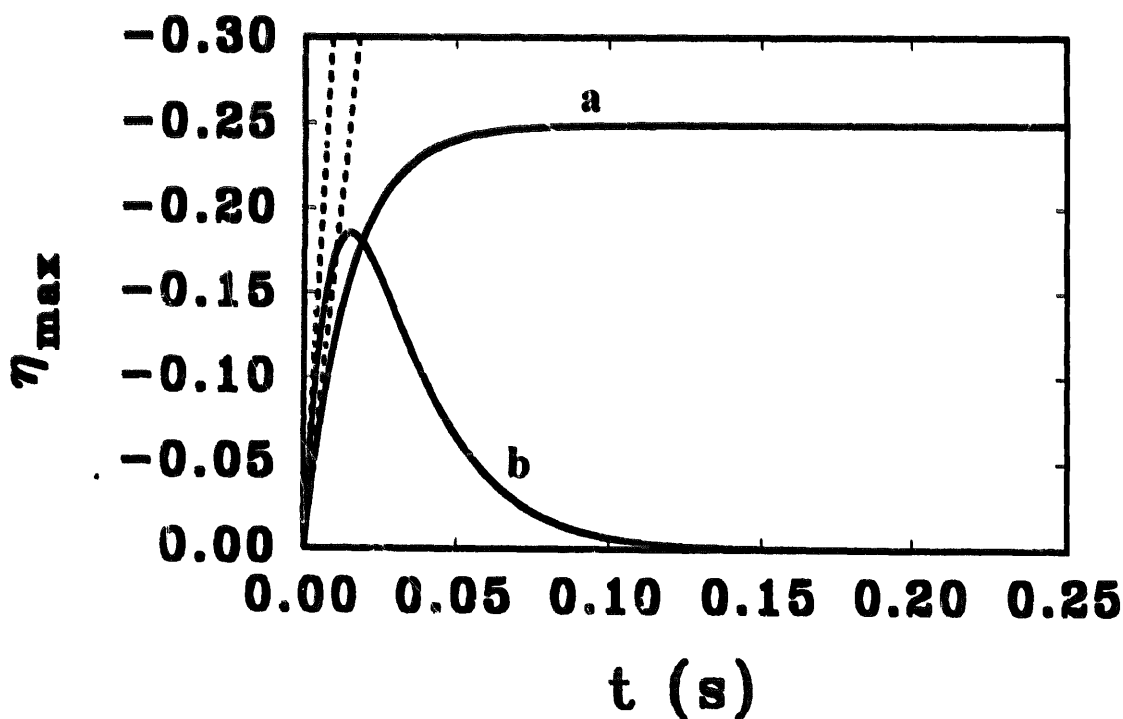


Fig. 6.7. Comparison between truncated steady state (a) and transient (b) NOE $R_{1M}^I = 50 \text{ s}^{-1}$. Other conditions as in Figs. 6.5 and 6.6. The dotted lines represent the initial slope (σ_{IJ} or $2\sigma_{IJ}$) in the two cases respectively.

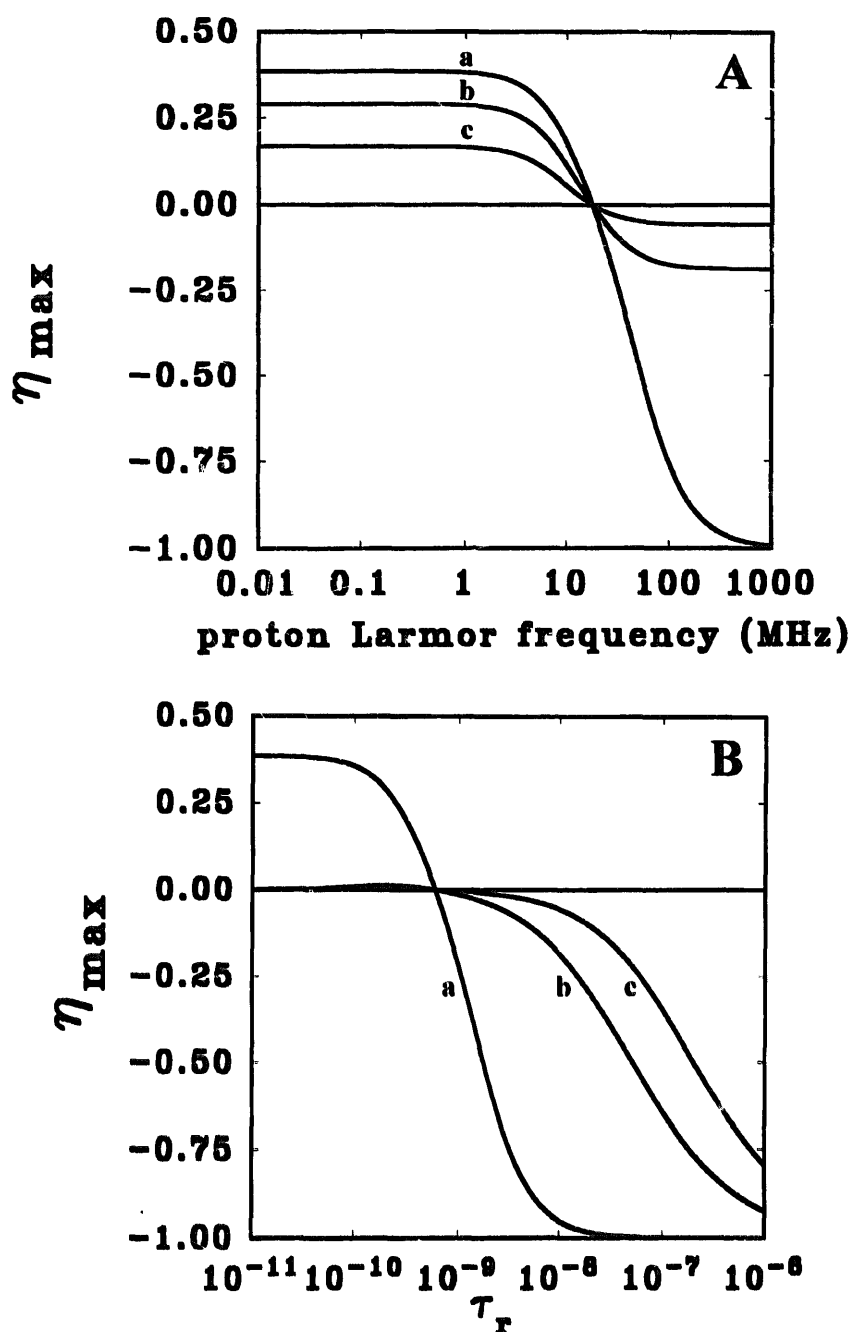


Fig. 6.8. Maximal intensity of transient NOE as a function of (A) magnetic field for $\tau_x = 10$ ns and (B) τ_r at a field of 300 MHz, for two nuclei at 1.8 Å distance ($\rho_{H(D)} = 23.6 \text{ s}^{-1}$ in the fast motion and 2.36 s^{-1} in the slow motion regime). Curves (a), (b) and (c) refer to a field-independent $R_{1M}^I = 0, 50$ and 200 s^{-1} respectively. Note that in the fast motion regime the maximal NOE for $R_{1M}^I = 0$ is 0.385 vs. 0.5 for steady state NOE (Fig. 6.2).

can now occur through cross relaxation and an intensity change on I can build up during the time t . This process is similar to that in a transient NOE experiment, with the difference that its extent depends on the rotating frame relaxation rate ρ_ρ

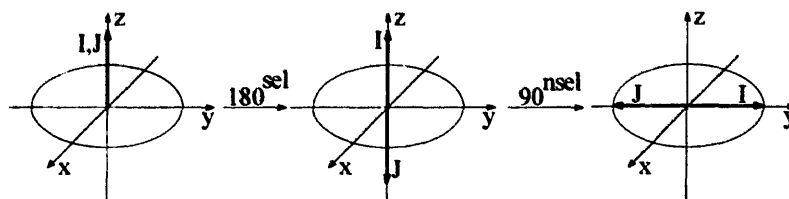


Fig. 6.9. A selective 180° pulse on signal *J* reverts its magnetization along the *z* axis while leaving the magnetization of *I* unaltered. A subsequent non-selective 90° pulse tilts the magnetization of *I* along *y* and that of *J* along *−y*.

and on the rotating frame cross relaxation rate σ_ρ . In analogy with Eqs. (6.5) and (6.6) we can write

$$\rho_{\rho I(J)} = \left(\frac{\mu_0}{4\pi}\right)^2 \frac{\hbar^2 \gamma_I^2 \gamma_J^2 J(J+1)}{30r_{IJ}^6} \left[\tau_c + \frac{9\tau_c}{1 + (\omega_{1I} + \omega_{1J})^2 \tau_c^2} + \frac{18\tau_c}{1 + \omega_I^2 \tau_c^2} + \frac{12\tau_c}{1 + (\omega_I + \omega_J)^2 \tau_c^2} \right] \quad (6.21)$$

$$\sigma_{\rho I(J)} = \left(\frac{\mu_0}{4\pi}\right)^2 \frac{\hbar^2 \gamma_I^2 \gamma_J^2 J(J+1)}{30r_{IJ}^6} \left[-\tau_c + \frac{9\tau_c}{1 + (\omega_{1I} + \omega_{1J})^2 \tau_c^2} + \frac{12\tau_c}{1 + \omega_I^2 \tau_c^2} \right] \quad (6.22)$$

where $\omega_{1I} = \gamma_I B_1$ and $\omega_{1J} = \gamma_J B_1$ are the Larmor frequencies at the spin locking field. It is important to note that, because $\omega_1 \tau_c$ is always smaller than unity, σ_ρ is always positive for every value of ω . Again in analogy with Eq. (6.19):

$$\eta_{I(J)} = \exp[-(\rho_\rho - D_\rho)t] [1 - \exp(-2D_\rho t)] \quad (6.23)$$

where, in analogy with Eq. (6.14)

$$\rho_\rho \equiv \frac{1}{2}(\rho_{\rho I} + \rho_{\rho J}) \quad D_\rho \equiv \frac{1}{2}[(\rho_{\rho I} - \rho_{\rho J})^2 + 4\sigma_{\rho I(J)}\sigma_{\rho J(I)}]^{1/2} \quad (6.24)$$

The ROE dependence on the spin lock time has the same profile as that of transient NOE, with the difference that the limiting values are 0.385 and 0.675 at the condition that $\omega_1 \tau_c \ll 1$ (see Fig. 6.10). It appears that the ROE is less convenient than the transient and steady state NOEs in the sense that the expected effect is smaller when all other conditions are the same. Another disadvantage in paramagnetic molecules is that it is difficult to spin lock all the signals in a broad spectral width, whereas it is simple to selectively spin lock a single signal. In order to spin lock two signals, separated by e.g. 1000 Hz, a B_1 field such that $\gamma B_1/2\pi \gg 1000$ Hz is needed. However, a large intensity of the r.f. requires high power irradiation and may cause overheating of the sample. This can be a serious drawback. An advantage of ROE is that the zero value for NOE never occurs. This may constitute a precious help for the measurement of dipolar interactions in small paramagnetic complexes. As in the fast motion limit of NOE, spin diffusion effects in ROE are quenched because of the positive value of σ_ρ . Another advantage of having a positive σ_ρ is that the dipole-coupled nuclei display positive ROEs, whereas signals connected through chemical

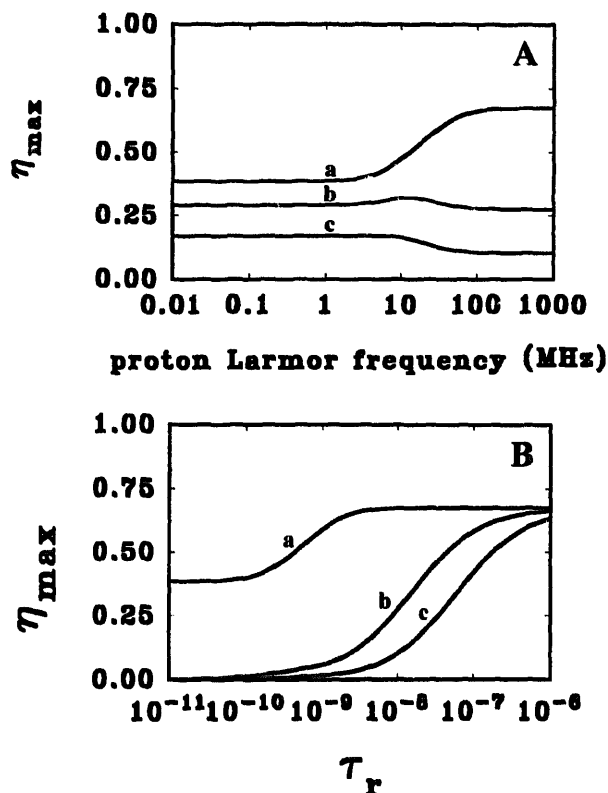


Fig. 6.10. Maximal intensity of the ROE as a function of (A) magnetic field for $\tau_r = 10$ ns and (B) τ_r at a field of 300 MHz, for two hydrogen nuclei at 1.8 Å distance. Curves (a), (b) and (c) refer to a field-independent $R'_{\rho M}$ (Eq. (3.18)) of 0, 50 and 200 s^{-1} respectively. For $R'_{\rho M} = 0$, the fast motion limit is the same as that of transient ROE; the slow motion limit is positive and equal to 0.675.

exchange always provide negative ROEs. This is because, in the presence of chemical exchange, when the J nuclei are aligned along $-y$, the I nuclei receive some $-y$ component and then the signal decreases in intensity. In the ROE experiment the I nuclei receive a y component as a result of σ_ρ being always positive.

References

- [1] A.W. Overhauser, Phys. Rev., 89 (1953) 689.
- [2] A.W. Overhauser, Phys. Rev., 92 (1953) 411.
- [3] J.H. Noggle and R.E. Schirmer, The Nuclear Overhauser Effect, Academic Press, New York, 1971.
- [4] D. Neuhaus and M. Williamson, The Nuclear Overhauser Effect in Structural and Conformational Analysis, VCH, New York, 1989.
- [5] R.D. Johnson, S. Ramaprasad and G.N. La Mar, J. Am. Chem. Soc., 105 (1983) 7205.
- [6] J. Granot, J. Magn. Reson., 49 (1982) 257.
- [7] L.B. Dugad, G.N. La Mar and S.W. Unger, J. Am. Chem. Soc., 112 (1990) 1386.
- [8] I. Bertini, C. Luchinat, L. Messori and M. Vasak, Eur. J. Biochem., 211 (1993) 235.
- [9] L. Banci, in L.J. Berliner and J. Reuben (Eds.), Biological Magnetic Resonance, Plenum, New York, Vol. 12, 1992.

- [10] I. Bertini, F. Capozzi, S. Ciurli, C. Luchinat, L. Messori and M. Piccioli, *J. Am. Chem. Soc.*, 114 (1992) 3332.
- [11] L. Banci, I. Bertini, C. Luchinat and M. Piccioli, *FEBS Lett.*, 272 (1990) 175.
- [12] L. Banci, I. Bertini, C. Luchinat and M.S. Viezzoli, *Inorg. Chem.*, 29 (1990) 1438.
- [13] I. Bertini, C. Luchinat and M. Piccioli, *Progr. NMR Spectrosc.*, 26 (1994) 91.
- [14] G. Wagner and K. Wüthrich, *J. Magn. Reson.*, 33 (1979) 675.
- [15] J.T.J. Lecomte, S.W. Unger and G.N. La Mar, *J. Magn. Reson.*, 94 (1991) 112.
- [16] A.A. Bothner-By, R.L. Stephens, J. Lee, C.D. Warren and R.W. Jeanloz, *J. Am. Chem. Soc.*, 106 (1984) 811.